Articles

Peripherin-2: An Intracellular Analogy to Viral Fusion Proteins†

T. C. Edrington, V,‡ R. Lapointe,‡ P. L. Yeagle,*,‡ C. L. Gretzula,§ and K. Boesze-Battaglia§

Department of Molecular and Cell Biology, University of Connecticut, Storrs, Connecticut 06269, and Department of Biochemistry, University of Pennsylvania School of Dental Medicine, Philadelphia, Pennsylvania 19104

Received August 31, 2006; Revised Manuscript Received January 15, 2007

ABSTRACT: The C-terminus of the intracellular retinal rod outer segment disk protein peripherin-2 binds to membranes, adopts a helical conformation, and promotes membrane fusion, which suggests an analogy to the structure and function of viral envelope fusion proteins. Nuclear magnetic resonance (NMR) data and fluorescence data show that a 63-residue polypeptide comprising the C-terminus of bovine peripherin-2 (R284−G346) binds to the membrane mimetic, dodecylphosphocholine micelles. High-resolution NMR studies reveal that although this C-terminal fragment is unstructured in solution, the same fragment adopts helical structure when bound to the micelles. The C-terminus may be a member of the class of intrinsically unstructured protein domains. Using methods developed for the G-protein coupled receptor rhodopsin, a model for the structure of the transmembrane domain of peripherin-2 was constructed. Previously published data showed that both peripherin-2 and viral fusion proteins are transmembrane proteins that promote membrane fusion and have a fusion peptide sequence within the protein that independently promotes membrane fusion. Furthermore, the fusion-active sequence of peripherin-2 exhibits a sequence motif that matches the viral fusion peptide of influenza hemagglutinin (HA). These observations collectively suggest that the mechanism of intracellular membrane fusion induced by peripherin-2 and the mechanism of enveloped viral fusion may have features in common.

Biological membrane fusion is central to fundamental cellular processes, including intracellular vesicle transport, entry of enveloped viruses into cells, endocytosis, exocytosis, and fertilization as well as the development and physiology of multicellular organisms. In these processes, two membranes fuse to become one, or one membrane reverses the process and becomes two.

Intracellular vesicle transport requires a protein complex including soluble *N*-ethylmaleimide-sensitive factor attachment protein receptors (SNAREs[1]) that play a central role in membrane targeting, attachment, and fusion (*1*, *2*). At a minimum, this membrane fusion process requires a v-SNARE and a corresponding t-SNARE in the opposing membrane. Whether the SNAREs are sufficient to promote lipid bilayer mixing in the final phase of membrane fusion or whether another factor is required is a matter of intense and un-resolved discussions (*3*).

Fusion of viral membranes with host cell membranes allows the penetration of the host cell cytoplasm by the viral nucleocapsid. Membrane fusion, required for enveloped viral entry into host cells, utilizes a fusion protein in the viral envelope to mediate the final steps of membrane fusion. Viral fusion proteins in the viral envelope support membrane fusion with the target membrane (*4*, *5*), and these viral fusion proteins are sufficient to induce membrane fusion when purified and reconstituted (*6*, *7*). For many viral fusion proteins, a segment of the protein has been identified as the fusion peptide. When this sequence is synthesized as a peptide, it independently promotes membrane fusion (*8*). Although viral fusion is mediated by a receptor on the host cell, actual membrane fusion requires a single viral fusion protein. No intracellular functional counterpart to the viral fusion protein has previously been identified.

Membrane fusion supports outer segment renewal in the vertebrate retinal rod photoreceptor cells. Membrane fusion between select disk membranes of the outer segment and the opposing plasma membrane initiates packet formation and shedding of old disks at the apical tip of the outer segment (*9*, *10*). Peripherin-2, a member of the tetraspanin family of integral membrane proteins, is an intracellular protein of the rod outer segment (ROS) disk that has been shown *in vitro* to be responsible for fusion between the disk membrane and the plasma membrane of the ROS (*11*, *12*). The tetraspanin family contains another member, CD9, that plays a role in sperm−egg fusion (*13*).

† This work was supported by USPHS Grant EY010420, E. Matilda Ziegler Vision Award, Vision Core Grant P30 EY001583, and an award from the Research Foundation of the University of Connecticut.

* To whom correspondence should be addressed. Phone: 860-486-5154. Fax: 860-486-4331. E-mail: yeagle@uconn.edu.

‡ University of Connecticut, Storrs.

§ University of Pennsylvania School of Dental Medicine.

[1] Abbreviations: CSI, chemical shift index; DPC, dodecylphosphocholine; GST, glutathione *S*-transferase; HA, hemagglutinin glycoprotein of influenza virus; NMR, nuclear magnetic resonance; SNARE, soluble *N*-ethylmaleimide-sensitive factor attachment protein receptors; TM, transmembrane segment.

10.1021/bi061820c CCC: $37.00
Published on Web 02/27/2007

A model for the transmembrane domain of peripherin-2 was developed in this report. The structure of the C-terminus of the protein was defined from high-resolution nuclear magnetic resonance (NMR) data. The behavior of the C-terminus, in conjunction with data previously reported for peripherin-2, reveals a remarkable correlation between peripherin-2 and viral fusion proteins, suggesting that peripherin-2 is one of the first intracellular membrane fusion proteins to be described that may function in a manner similar to that of viral fusion proteins. Both peripherin-2 and viral fusion proteins are transmembrane proteins, both promote membrane fusion, and both have a fusion peptide sequence within the protein. Fusion peptides from both proteins independently promote membrane fusion. Fusion peptides from peripherin-2 and viral fusion proteins bind to membrane mimetics and become helical. Collectively, these observations suggest that the mechanism of intracellular membrane fusion induced by peripherin-2 and the mechanism of enveloped viral fusion may have features in common.

MATERIALS AND METHODS

Materials. Dodecylphosphocholine (DPC) was obtained from Avanti Polar Lipids (Alabaster, AL). $^{15}NH_4Cl$ was obtained from Sigma (St. Louis, MO).

Expression and Purification of GST-Peripherin-2. The glutathione *S*-transferase (GST) fusion protein encoding the 63 C-terminal amino acids (PerCter) of bovine peripherin-2 (sequence = ^{284}RYLHTALEGMANPEDPECESEGWLLEKSVPETWKAFLESVKKLGKGNQVEAEGEDAGQAPAAG^{346}) was produced. The generation of this construct and the expression and purification of this fusion protein have been described previously (*14*). Briefly, *E. coli* BL21 (DE3) cells transformed with the GST-PerCter construct in a pGEX-2T vector (*14*, *15*) were grown in M9 media supplemented with ^{15}N-labeled $^{15}NH_4Cl$ (1 g/L; 20 mM) containing 50 mg/mL ampicillin. Cells were harvested 2 h after induction with 0.1 mM of isopropyl-β-D-thiogalactopyranoside (IPTG), spun down, resuspended, and sonicated in cold PBS at pH 7.3, 8 mM DTT, 0.1% Triton X-100, and 0.2 mM AEBSF. Cellular debris was removed by centrifugation, and the supernatant was loaded onto two stacked Amersham 5 mL GST affinity columns (Amersham) for FPLC. The supernatant was loaded at a flow rate of 2 mL/min at 0.3 pSA. The purified GST-PerCter was cleaved with 400 U of thrombin (10 U of thrombin per mg of protein) and concentrated for use in NMR studies. Specificity was monitored by Western blots (Figure 1A) and purification by silver stained SDS−PAGE (Figure 1B). For NMR studies, we routinely harvested 5−7 mg of pure ^{15}N-labeled PerCter from 10 L of *E. coli*. The polypeptide was concentrated using a centricon (Millipore) 3,000 MW cutoff filter and dialyzed against 20 mM $NaPO_4$ at pH 6.5, 50 mM NaCl, 100 μM DTT, 10 μM EDTA, 0.2 mM AEBSF, and 0.001% NaN_3. Residual Triton X-100 was removed with Bio-Beads SM2 from Bio-Rad (Hercules, CA) to yield the pure product. The final concentration of PerCter was determined by measuring the absorbance at 280 nm using a molar extinction coefficient (derived empirically as described (*16*)) of 12,780 M^{-1} cm^{-1}.

Fluorescence Experiments. Steady-state fluorescence utilized an L-format Perkin-Elmer (Wellesley, MA) LS 50B luminescence spectrometer. For all measurements, a 10 mm path length Spectrosil quartz cuvette from Starna Cells, Inc. (Atascadero, CA) was used. Spectra of 10 μM PerCter in 20 mM $NaPO_4$ at pH 7.4, 50 mM NaCl, and 100 μM DTT, with and without 293 mM DPC, were recorded. DPC has a critical micelle concentration of 1 mM (*17*, *18*). Samples were excited at a wavelength of 295 nm, and emission spectra were recorded from 310−450 nm. The excitation and emission band passes were 3 and 5 nm, respectively. All spectra were corrected for background from the buffer. Spectra were smoothed using the moving average algorithm provided with Perkin-Elmer's FLWinLab software (over 5 points).

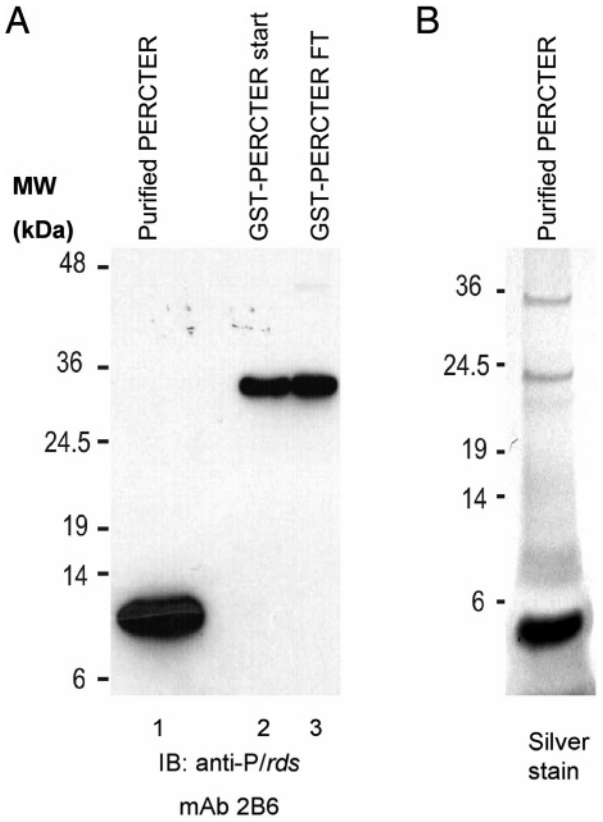

FIGURE 1: Purification of ^{15}N-labeled bovine PerCter. The GST-peripherin-2 polypeptide was expressed and isolated from *E. coli* as described in Materials and Methods. The resultant polypeptide was bound to glutathione beads, washed, and cleaved with thrombin. The purified PerCter was separated from the thrombin and GST by dialysis (Centricon, 30 kDa MW cutoff) as described in detail in Materials and Methods. (A) Three polypeptide fractions of GST-PerCter starting material, GST-PerCter wash, and the purified PerCter were isolated, separated by SDS−PAGE, and the proteins transferred to nitrocellulose and immunoblotted with anti-peripherin-2 mAb 2B6. Lane 1, purified peripherin-2 C-terminus; lane 2, GST-peripherin-2 C-terminus isolated from *E. coli*; lane 3, unbound GST-peripherin-2 C-terminus recovered after the wash step. (B) Silver stain of purified peripherin-2 C-terminus.

Modeling Methods. A Kyte−Doolittle plot (*19*) was developed from the primary sequence of bovine peripherin-2 to identify the sequences most likely to form transmembrane segments. Four hydrophobic regions of the sequence (Figure 2A) were identified as putative transmembrane regions. The boundaries of the four transmembrane regions of this tetraspanin were then defined. A search for clusters of charged residues often found at the hydrophobic/hydrophilic interface of membranes and the location of tryptophans often found at the same interface (*20*) helped define those

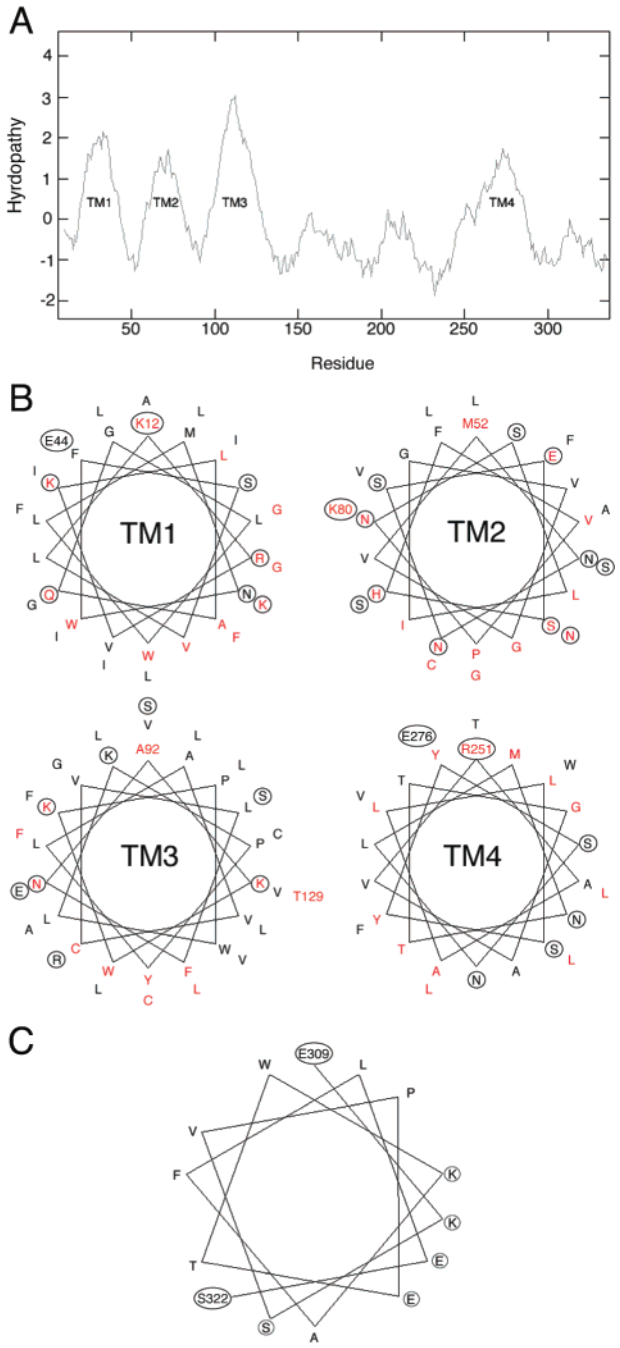

FIGURE 2: Modeling the peripherin-2 transmembrane domains. (A) Kyte−Doolittle plot for bovine peripherin-2, using a window function of 19 (http://occawwlonline.pearsoned.com/bookbind/pubbooks/bc_mcampbell_genomics_1/medialib/activities/kd/kyte-dolittle.htm). (B) Helical wheels for TM1, TM2, TM3, and TM4 were constructed for the sequences shown in Table 1 and derived from peripherin-2 as described in the text. Conserved residues are colored red and polar residues are circled. The dominant clustering of these conserved, and the polar residues on one helical face can be readily seen. (C) Helical wheel for the structured region of the PerCter with polar residues circled, showing amphipathic character.

boundaries for peripherin-2. Four idealized helices were built *in silico* (Sybyl software, Tripos, St. Louis) to represent these transmembrane segments TM1, TM2, TM3, and TM4 (Table 1). To organize these helices into a bundle, the method of Baldwin was used (*21*) as follows. BLAST searches identified conserved residues, and polar residues were located. Helical wheel analysis of TM1, TM2, and TM4 revealed that the conserved and polar residues were located

Table 1: Sequences of Transmembrane Domains of Peripherin-2

TM1	KRVKLAQGLWLMNWFSVLAGIIIFGLGLFLKIE
TM2	MNNSESHFVPNSLIGVGVLSCVFNSLAGK
TM3	AKWKPWLKPYLAVCVLFNVVLFLVALCCFLLRGSLEST
TM4	RAALLSYYSNLMNTTFAVTLLVWLFE

on one face of the helix, dominating that face from one end to the other and demarking a surface relatively uniform in width throughout. For TM3, a 3D representation of the sequence as a helix showed that the conserved and polar residues defined a surface that was contiguous but was not uniform in width from one end to the other of the helix. The helical faces containing conserved and polar residues were then oriented toward each other, according to Baldwin's rules, that is, that conserved and polar residues in a transmembrane helical bundle were most likely to be found in contact with residues from other helices in the transmembrane bundle and least likely to be found in contact with the membrane−lipid matrix.

Nuclear Magnetic Resonance. All NMR studies utilized a Varian 600 MHz instrument equipped with a Cold Probe and were performed at 25 °C. The sequence-specific assignment of the PerCter was carried out using standard methods to establish scalar, through-bond connectivity in proteins. The NMR samples used in the studies contained either 1 mM ^{15}N-PerCter or 1 mM ^{15}N-PerCter in the presence of 293 mM DPC (>100:1 DPC/PerCter mole ratio) in 20 mM $NaPO_4$ at pH 6.5, 50 mM NaCl, 100 μM DTT, 10 μM EDTA, 0.2 mM AEBSF, 0.001% NaN_3, and 10% D_2O. All data were processed using NMRPipe (*22*) and analyzed using Sparky v3.110 software (http://www.cgl.ucsf.edu/home/sparky/).

For the analysis of the ^{15}N-PerCter in solution without DPC, a combination of 2D ^{1}H-^{15}N HSQC, ^{1}H-^{1}H NOESY (τ = 150 and 300 ms), ^{1}H-^{1}H TOCSY (τ = 30, 45, and 60 ms), with 3D ^{1}H-^{15}N HSQC-TOCSY (τ = 45 and 75 ms) and ^{1}H-^{15}N HSQC-NOESY (τ = 100 and 400 ms) data were utilized. ^{1}H-^{15}N HSQC data were acquired with 2048 points in the ^{1}H dimension, 128 points in the ^{15}N dimension, and averaged over 16 transients. ^{1}H-^{1}H NOESY and ^{1}H-^{1}H NOESY data were acquired with 2048 points in the first ^{1}H dimension and 256 points in the second ^{1}H dimension, and averaged over 32 transients. ^{1}H-^{15}N HSQC-NOESY and ^{1}H-^{15}N HSQC-TOCSY spectra were acquired with 2048, 32, and 32 points in the ^{1}H dimension, second ^{1}H dimension, and ^{15}N dimension, respectively, while being averaged over 32 transients.

For the assignment of the ^{15}N-PerCter in solution in the presence of DPC, 2D ^{1}H-^{15}N HSQC, along with 3D ^{1}H-^{15}N HSQC-TOCSY (τ = 45 and 75 ms) and ^{1}H-^{15}N HSQC-NOESY (τ = 100 and 400 ms) data were collected. ^{1}H-^{15}N HSQC data were acquired with 2048 points in the ^{1}H dimension and 128 points in the ^{15}N dimension, and averaged over 16 transients. ^{1}H-^{15}N HSQC-NOESY and ^{1}H-^{15}N HSQC-TOCSY spectra were acquired with 2048, 32, and 32 points in the ^{1}H dimension, second ^{1}H dimension, and ^{15}N dimension, respectively, while being averaged over 32 transients.

The transverse relaxation (T_2) analysis was performed as described (*23*) with a slight modification. Briefly, ^{15}N relaxation data were recorded utilizing experiments from the Varian BioPack. A series of ^{1}H-^{15}N HSQC spectra of 1 mM

^{15}N-labeled PerCter with 293 mM DPC (>100:1 DPC/PerCter mole ratio) in the respective buffer were recorded at 25 °C with relaxation delays of 10, 30, 50, 70, 90, 110, 190, and 250 ms. Data were collected in an interleaved manner with alternating long−short relaxation periods to minimize fluctuations in peak intensity because of instrument instability. The ^{1}H-^{15}N HSQC spectra were acquired with 2048 points in the ^{1}H dimension, 200 points in the ^{15}N dimension, and averaged over 16 transients. From the respective spectra, the peak height of each distinct and identifiable amino acid resonance was obtained. T_2 values were derived from curving fitting to a one-phase exponential decay using Prism 3.0a software from GraphPad Software Inc. (San Diego, CA).

RESULTS

Peripherin-2 is linked to the process of disk renewal through its role in promoting membrane fusion between disks and the plasma membrane. A 63-residue fragment from the carboxyl terminus of peripherin-2 or PerCter promotes membrane destabilization and model membrane fusion (*24*−*26*), indicating that the C-terminus carries the membrane fusion function. Both C-terminal gain- and loss-of-fusion function mutants have been characterized (*27*). The structure of PerCter in the presence of membranes is required to mechanistically understand the role peripherin-2 plays in membrane fusion. The structure of the C-terminus is unknown; one hypothesis stimulated by the analogy with viral fusion proteins is that this fusion peptide becomes helical in the presence of membranes, as do many viral fusion peptides. The following experiments test this hypothesis.

NMR provides a means to define structure on a molecular scale. Therefore, an expression system for the bovine peripherin-2 C-terminus was developed (Materials and Methods). This 63-residue polypeptide fragment was expressed in minimal media with ^{15}N-labeled NH_4Cl as the sole nitrogen source and subsequently purified. As a control, an NMR structure investigation was initiated on PerCter in solution. Analytical ultracentrifugation demonstrated that this fragment of peripherin-2 was a monomer in solution (*28*), making it suitable for NMR studies. ^{15}N-labeling enabled multidimensional NMR studies. A ^{1}H-^{15}N HSQC of PerCter in solution appears in Figure 3A. The lack of dispersion in the ^{1}H-^{15}N HSQC suggested that the PerCter was intrinsically unstructured in solution. This was investigated further with a set of multidimensional experiments. From these experiments, only a partial sequence-specific assignment was possible, and the chemical shifts were consistent with random coil chemical shifts. Analysis of the NOESY data revealed almost no long-range (nonadjacent) NOEs (data not shown). The NMR data, therefore, supported the conclusion that this fragment of peripherin-2 was intrinsically unstructured in the absence of membranes.

Previous analyses of fusogenic peptides from viral fusion proteins have found that fusion peptides adopted helical structures in the presence of membrane mimetics (*29*−*31*). Because optical and NMR studies in the presence of membrane vesicles, even with small vesicles, are plagued with experimental problems due to vesicle size, detergent micelles are used as a membrane mimetic because of their much smaller size. Detergent micelles provide an architecture similar to that of membranes except for the short radius of curvature of the structure. The latter is a distinct advantage for NMR experiments because peptides bound to phospholipid vesicles cannot be readily studied by high-resolution NMR because of the long rotational correlation times (τ_c) of the vesicle. However, caution is appropriate because of the physical differences that the highly curved surface may impart to the system.

Initial studies were designed to determine if PerCter bound to detergent micelles as a membrane mimetic. DPC was chosen for the detergent because it was suitable for both the optical and the NMR experiments. The PerCter contains two tryptophan residues W306 and W316. The previously reported fusion peptide region PP-5 (*32*) contains W316. To investigate whether the PerCter is associated with the membrane-mimetic DPC micelles at or near the PP-5 fusion region, we examined the intrinsic tryptophan fluorescence of the PerCter in the presence of DPC micelles. Upon the introduction of DPC micelles (Figure 4), the spectrum of the PerCter tryptophan fluorescence emission displays a significant blue shift (average, 10.0 nm ± 3.0 nm) and a marked increase in fluorescence intensity (average $F_{DPC}/F = 2.65 \pm 0.13$). These results strongly suggested that at least one of these two tryptophan residues was sequestered from the polar solvent within the DPC micelle interface.

Because the fluorescence data suggested that the PerCter bound to DPC micelles, an ^{1}H-^{15}N HSQC-NOESY experiment was performed on ^{15}N-labeled PerCter in the presence of DPC micelles. The NOE data were examined for evidence of NOEs between the PerCter and the micelles. Figure 3D shows NOEs between the tryptophan side chains of PerCter and methylenes from the dodecyl group of DPC, observed at both mixing times (100 and 400 ms). In the absence of DPC, these NOEs were not present (Figure 3B). These data revealed a penetration of the micelle by the tryptophans of PerCter and confirmed that this peripherin-2 C-terminal fragment bound to this membrane mimetic. These two independent experimental approaches established that PerCter bound to the DPC micelles, consistent with previous studies showing that a much smaller fusion peptide domain (residues 312−326) bound to membranes (*33*).

This system was studied further by NMR to determine the structural effects on the peripherin-2 fragment binding to the membrane mimetic. Multidimensional experiments were utilized to obtain a sequence-specific assignment (Materials and Methods). These chemical shifts are listed in the Table in Supporting Information. For a very limited set of resonances, a second set of peaks was observed, but the intensities were too weak to analyze. An ^{1}H-^{15}N HSQC of this system appears in Figure 3C. A greater dispersion in the peaks was noted compared to those of the peptide in the absence of detergent micelles, consistent with an increase in structure in this protein fragment in the presence of DPC micelles.

A qualitative comparison of the ^{1}H-^{15}N HSQC of the free PerCter and the ^{1}H-^{15}N HSQC of the PerCter in the presence of DPC micelles revealed a pattern of chemical shift changes. Figure 5A shows squares at the positions of residues for which the ^{1}H-^{15}N HSQC peak was significantly (>0.02 ppm) shifted between the two experiments. In some cases, the amino acid peak in the spectrum of the protein fragment alone was not identifiable because of spectral overlap but

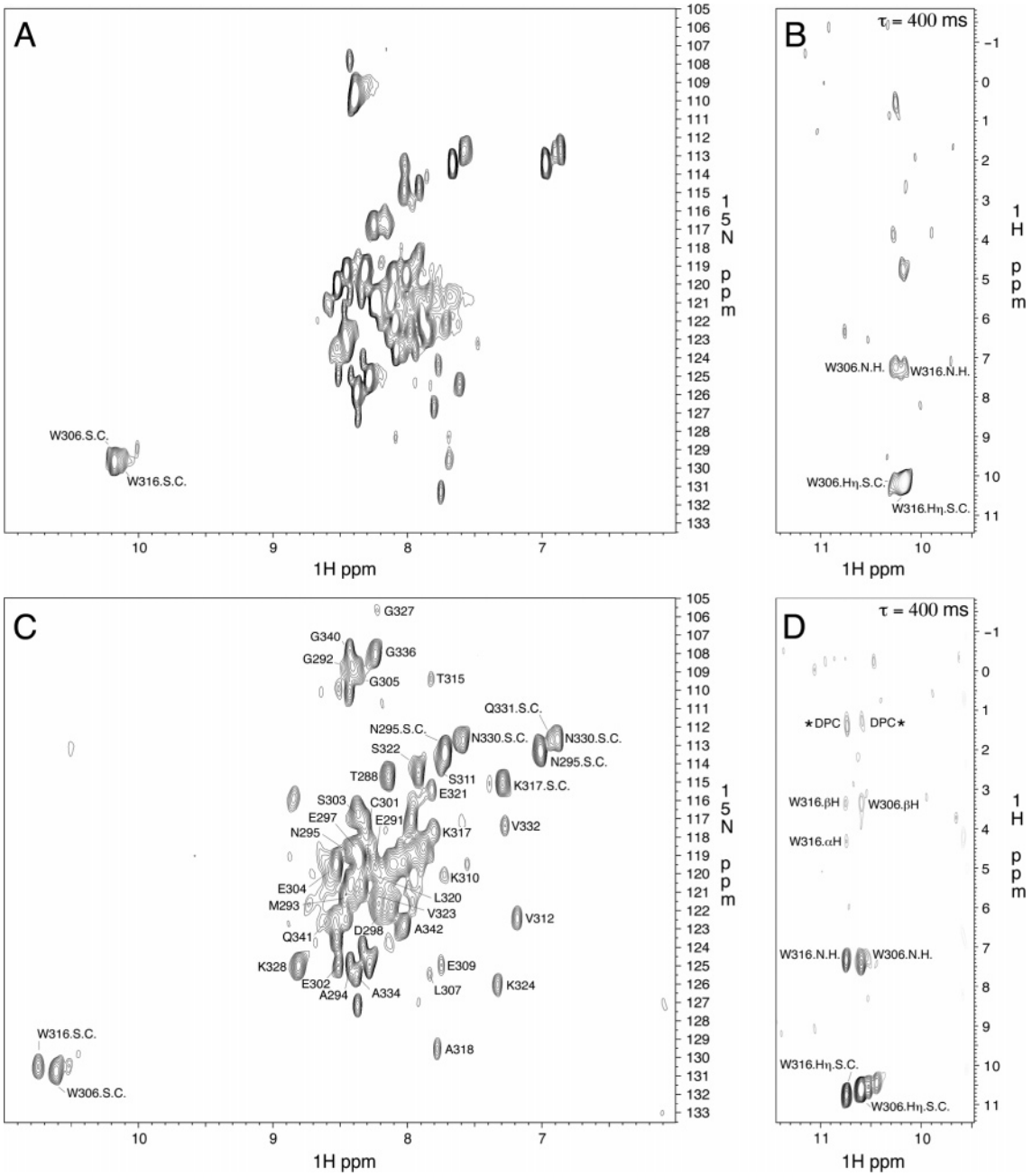

FIGURE 3: NMR spectra of ^{15}N-labeled PerCter. (A) ^{1}H-^{15}N HSQC of 1 mM PerCter free in solution; (B) ^{1}H-^{15}N HSQC-NOESY experiment showing the W306 and W316 side chain NOEs of the free PerCter; (C) ^{1}H-^{15}N HSQC of 1 mM PerCter with 293 mM DPC (>100:1 DPC/PerCter mole ratio); (D) ^{1}H-^{15}N HSQC-NOESY experiment showing NOEs between W306 and W316 from the PerCter and the methylenes of DPC.

became readily identifiable upon the addition of DPC. Such residues were denoted as being significantly changed between the two relative spectra. This analysis identifies a sequence in the middle of the fragment that is influenced by the presence of the DPC micelles.

Using the chemical shift index (CSI) for amino acid alpha protons, calculated as a difference in ppm from reference values (*34*), and the sequence specific chemical shift assignments for PerCter in the presence of DPC micelles, the propensity for secondary structure was analyzed and the result presented in Figure 5A, underneath the chemical shift changes induced by the DPC micelle. The pattern of negative peaks (demonstrating upfield shifts in the Cα proton resonances relative to the random coil CSI values) was consistent with the presence of the helix in the middle of the peptide. This was the same region of the sequence in which changes in chemical shifts were observed between the ^{1}H-^{15}N HSQC of the free peptide and the ^{1}H-^{15}N HSQC of the peptide bound to DPC micelles, which can, therefore, be linked to the conformational change from intrinsically unstructured to a partially structured state.

Further evidence for a helical conformation when bound to DPC micelles was found in the NOESY data. Several long-range NOEs were observed in the ^{1}H-^{15}N HSQC-NOESY spectrum of PerCter in the presence of DPC micelles. These are also graphed in Figure 5A to compare them with the CSI analysis and the changes in ^{15}N-HSQC chemical shifts induced by the micelles. Many of these NOEs are between residues three and four positions in sequence distance. Such a pattern of NOEs is consistent with the

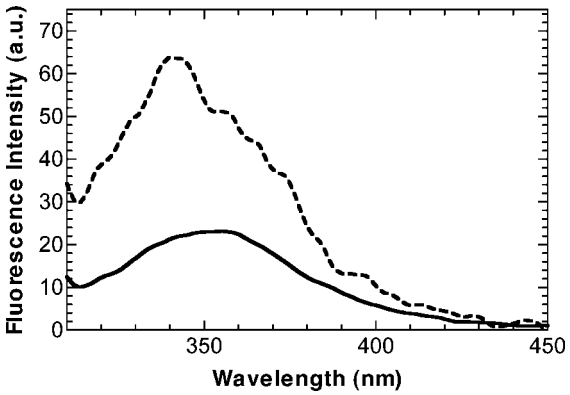

FIGURE 4: Representative steady-state fluorescence spectra of 10 μM PerCter (—) and 10 μM PerCter upon the addition of 293 mM DPC (---). The samples were excited at 295 nm.

formation of helical structure in the presence of the DPC micelles, consistent with the CSI analysis. Attempts were made to fold the structure on the basis of these NOEs, but while helix-like turns were observed as suggested by the pattern of NOEs, the data were too sparse to adequately define a stable structure.

The above experiments described a conformational change of the C-terminal fragment of peripherin-2 when in the presence of a membrane mimetic but do not define what part of the C-terminus actually binds to the DPC micelle. Therefore, peptide backbone relaxation data (T_2) were obtained as described in Materials and Methods to evaluate the effect of the binding to the micelle on the dynamics of the PerCter. T_2 relaxation data are sensitive to the correlation time. The complex of PerCter (7 kDa) with a DPC micelle (19 kDa (*35*)) has a longer τ_c compared to that of the PerCter alone. The longer τ_c will shorten T_2. Therefore, the region of the PerCter associated with the micelle will exhibit reduced T_2 values compared to those of regions of the PerCter not associated with the micelle. (The latter have modes of motion independent of micelle rotational diffusion, which will partially average interactions that contribute to T_2.) T_2 data were obtained for many of the peaks in the ^{15}N-edited HSQC and are reported in Figure 5B. The T_2 for W306 and W316 were too short to measure in this experiment. T_2 in the region between 306 and 316 was, on average, substantially shorter than T_2 in the flanking regions. The results revealed a region between W306 and W316 in PerCter that showed a considerable reduction in T_2. This reduction in T_2 was consistent with an increase in τ_c expected for PerCter upon leaving solution and binding to a detergent micelle.

To put these structural data in the context of the whole peripherin-2 molecule, a model was constructed for the transmembrane helices of peripherin-2 using the same approach originally reported by Baldwin for the G-protein coupled receptor, rhodopsin (*21*). Putative transmembrane segments were identified (as described in Materials and Methods). Helical wheel analysis revealed that these segments, if α-helical, clustered conserved residues and polar residues on one face of each helix (Figure 2B). The sequences of the putative transmembrane segments were used to build α-helices *in silico*. To model the transmembrane bundle for this protein, these helices were packed such that the conserved/polar surfaces were in contact with other TMs and not with the lipid matrix. In this bundle, three helices could be readily oriented roughly perpendicular to the membrane surface, successfully bringing all of the appropriate surfaces in contact. However, because of the nonuniform organization of the surface of TM3, TM3 required a tilt with respect to the other three TMs to allow full contact of the conserved/polar surface of TM3 with the corresponding surfaces of the other TM in the bundle. This orientation of TM3 gained support from data for another tetraspanin, human CD81. A crystal structure of the large loop connecting TM3 with TM4 from human CD81 (*36*), which corresponds to the intradiskal EC2 domain from peripherin-2 (*37*), contained helices at the amino and carboxyl terminal of this fragment. These helical segments likely represent a portion of TM3 and TM4 and thus describe the relative orientations of the two transmembrane helices to which the loop was attached. The orientation was consistent with the model developed using Baldwin's approach. Finally, the longitudinal translational orientation of the helices was organized such that the tryptophans were located as much as possible in lateral planes (roughly perpendicular to the long axis of the helical bundle). Figure 6 shows the helical bundle as modeled. Attached to the model of the helical bundle is the PerCter with the helical segment identified from the experimental NMR data (obtained in the presence of the membrane mimetic, DPC).

DISCUSSION

The structural data presented here of the PerCter free in solution describe an intrinsically unstructured C-terminal fragment of peripherin-2 (R284 to G346). Because this 63-residue fragment represents the C-terminal domain, one can conclude that the C-terminus of the native protein is intrinsically unstructured in the absence of any interactions, in agreement with the previous prediction (*28*). However, peripherin-2 is an integral membrane protein with membrane fusion activity. Therefore, the structural influence of membrane surfaces in close proximity needs to be understood.

The data revealed that the PerCter bound to the membrane mimetic, DPC micelles, and adopted a helical structure when bound. The tryptophan fluorescence data and intermolecular NOE data between W306 and W316 and the detergent molecules showed that PerCter bound to the DPC micelles. Residues E309−S322 showed CSI indicative of helix formation, and residues E304−G327 showed some long-range NOEs consistent with helix formation. This conclusion was consistent with previous circular dichroism data (*26*).

Relaxation data suggested which portion of the PerCter was in contact with the DPC micelle. The T_2 experiments demonstrated a substantial reduction in T_2 between W306 and W316. The reduction in T_2 was consistent with that portion of PerCter binding to the surface of the DPC micelle and adopting the overall τ_c of the micelle as the dominant correlation time for transverse relaxation.

All, or nearly all, of the PerCter bound to the micelle. The spectra of the PerCter in the presence of DPC micelles were devoid of any peaks due to the free 63-mer. Therefore, all or nearly all, of the PerCter was bound. This is reasonable because the detergent was in excess of the PerCter. While bound, the PerCter may adopt more than one conformation. Multiple peaks were observed for each tryptophan side chain, indicative of two environments and/or conformations while bound.

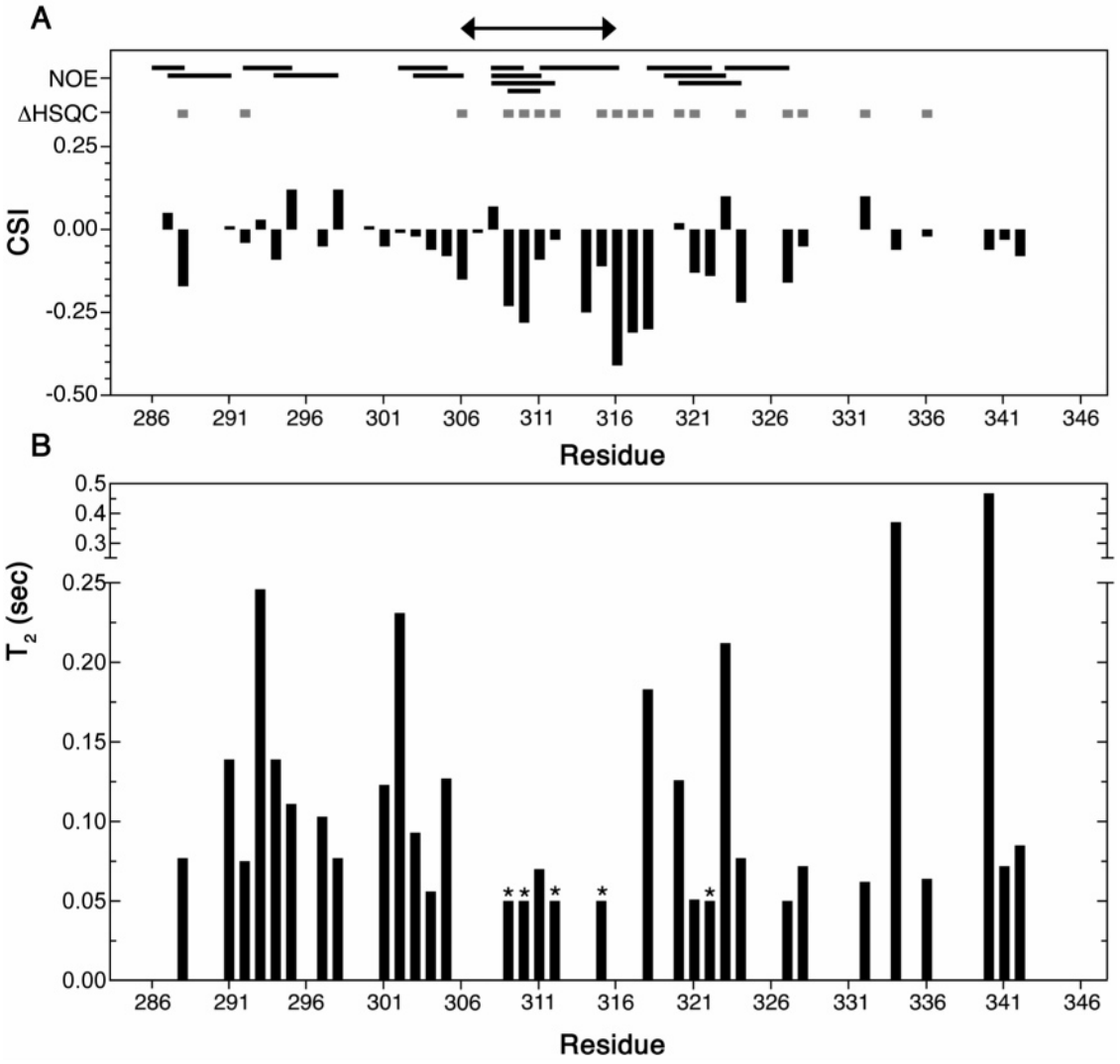

FIGURE 5: Results of NMR-based structural and dynamic analyses of the PerCter. The large arrow above the Figure denotes the region between W306 and W316. (A) CSI for Cα^{1}H chemical shifts, calculated as a difference in ppm from reference random-coil values (*34*) and plotted as a function of sequence for the PerCter in the presence of DPC micelles; ΔHSQC, residues exhibiting significant (>0.02 ppm) chemical shift changes in the ^{1}H-^{15}N HSQC spectrum of the PerCter in the presence of DPC compared to the ^{1}H-^{15}N HSQC spectrum of the peptide alone; NOE, plot of long-range NOEs as described in the text with the bar connecting residues showing inter-residue NOEs. (B) Sequential transverse relaxation rate (T_2) of each assigned residue in the PerCter; (∗) Residues for which T_2 was <0.05 s (exact values undefined because of the time domain of the experiment). Additionally, a more slowly relaxing and unassigned component was observed near S322.

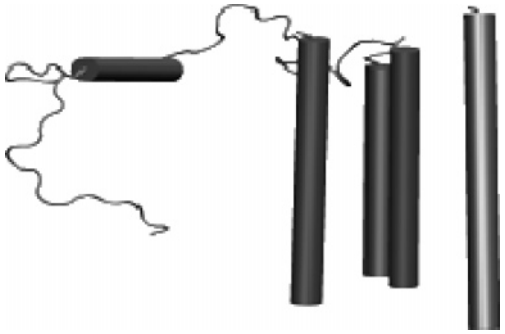

FIGURE 6: Model of the peripherin-2 transmembrane domain developed as described in the text with the C-terminal segment derived from the NMR data in the presence of the membrane mimetic DPC. The helical segment in the C-terminal portion derives from the experimental data presented in this article. The transmembrane helical bundle is modeled as described in the text using the procedure of Baldwin (*21*).

Collectively, these data suggest that the segment from approximately W306 to W316 binds to membrane surfaces and that the sequence from E309 to S322 tends to form a helical structure when bound to the DPC micelle. As a helix, this sequence is strongly amphipathic (Figure 2C), consistent with its surface activity, and likely forms approximately four helical turns. A model, based on the experimental data of the interaction of the C-terminus of peripherin-2 with the DPC micelle, suggests that the two tryptophans anchor the PerCter to the surface by intercalating between the lipid headgroups and occupying the interfacial region (between the hydrophobic interior and the polar headgroups) favored by tryptophans (*20*).

These observations link the C-terminus of peripherin-2 with other proteins that contain a portion of sequence that is intrinsically unstructured. Intrinsically unstructured proteins have attracted considerable interest recently, particularly because such behavior allows the same portion of the protein to interact with multiple, distinct partners and adopt specific structures with each (*38*−*40*). The C-terminus of peripherin-2 is known to bind to multiple, distinct partners (*41*−*44*).

Therefore, the intrinsically unstructured character that has been observed in this study may be the foundation for the mechanism by which peripherin-2 interacts with those multiple, distinct partners.

The tendency of the C-terminus of peripherin-2 to adopt a helical structure in the presence of membrane mimetics recalls the behavior of viral fusion proteins. Fusion peptides from viral fusion proteins also become helical when bound to membranes or membrane mimetics, such as fusion peptides from gp41 (*29*), influenza HA (*30*), and the EnvA fusion protein of avian sarcoma leukosis virus (*31*). Importantly, the same portion of the C-terminus of peripherin-2 that binds to membrane mimetics and becomes helical also promotes membrane fusion (*12*). In particular, a peptide comprising residues V312 to L326 promotes membrane fusion in the absence of the remainder of the protein. This observation also recalls the behavior of viral fusion peptides from viral fusion proteins.

Finally, there is an interesting sequence similarity between the portion of the C-terminus of peripherin-2 responsible for fusion and viral fusion peptides. In particular, a consensus sequence for the viral fusion peptide from influenza (N-terminal region of HA-2) can be derived from a comparison of the sequences from six influenza strains: phW-phhhp, where p is a polar or charged residue, h is a hydrophobic residue, and W is tryptophan (*45*, *46*). The sequence of peripherin-2 from 314 to 321 matches that consensus sequence from influenza.

The functional analogy between an intracellular membrane protein that promotes membrane fusion, peripherin-2, and viral fusion proteins from enveloped viruses is worth noting. Both types of proteins are integral membrane proteins. Both types of proteins promote membrane fusion independent of other protein factors. Both also require cofactors for the optimization of fusion, likely through binding to a receptor. Both kinds of proteins have a fusion peptide as part of their sequence. The PerCter and viral fusion peptides promote membrane fusion separate from the remainder of the protein. These new data show that the fusion peptide of peripherin-2, the PerCter, binds to membrane mimetics, as do viral fusion peptides. Furthermore, upon binding to membrane mimetics, the PerCter adopts a helical structure, as do many viral fusion peptides. Therefore, although differences do exist between peripherin-2 and viral fusion proteins (peripherin-2 is a tetraspanin and viral fusion proteins have only one transmembrane segment), the similarities are striking and extensive. These similarities suggest that some features of the membrane fusion mechanism may be the same between the intracellular membrane fusion promoted by peripherin-2 and viral membrane fusion promoted by viral fusion proteins.

SUPPORTING INFORMATION AVAILABLE

Chemical shift assignment table for PerCter. This material is available free of charge via the Internet at http://pubs.acs.org.

REFERENCES

1. Subramaniam, V. N., Peter, F., Philp, R., Wong, S. H., and Hong, W. (1996) GS28, a 28-kilodalton Golgi SNARE that participates in ER-Golgi transport, *Science 272*, 1161−1163.
2. Ungermann, C., and Langosch, D. (2005) Functions of SNAREs in intracellular membrane fusion and lipid bilayer mixing, *J. Cell Sci. 118*, 3819−3828.
3. Chen, X., Arac, D., Wang, T. M., Gilpin, C. J., Zimmerberg, J., and Rizo, J. (2006) SNARE-mediated lipid mixing depends on the physical state of the vesicles, *Biophys. J. 90*, 2062−2074.
4. Scheid, A., and Choppin, P. W. (1974) Identification of biological activities of paramyxovirus glycoproteins. Activation of cell fusion, hemolysis, and infectivity by proteolytic cleavage of an inactive precurser protein of Sendai virus, *Virology 57*, 475−490.
5. Garoff, H., Frischauf, A. M., Simons, K., Lehrach, H., and Delius, H. (1980) Nucleotide sequence of cdna coding for Semliki forest virus membrane glycoproteins, *Nature 288*, 236−241.
6. Eidelman, O., Schlegel, R., Tralka, T. S., and Blumenthal, R. (1984) pH-dependent fusion induced by vesicular stomatitis virus glycoprotein reconstituted into phospholipid vesicles, *J. Biol. Chem. 259*, 4622−4628.
7. Nussbaum, O., Lapidot, M., and Loyter, A. (1987) Reconstitution of functional influenza virus envelopes and fusion with membranes and liposomes lacking virus receptors, *J. Virol. 61*, 2245−2252.
8. Haque, M. E., Koppaka, V., Axelsen, P. H., and Lentz, B. R. (2005) Properties and structures of the influenza and HIV fusion peptides on lipid membranes: implications for a role in fusion, *Biophys. J. 89*, 3183−3194.
9. Matsumoto, B., and Besharse, J. C. (1985) Light and temperature modulated staining of the rod outer segment distal tips with Lucifer Yellow, *Invest. Ophthalmol. Visual Sci. 26*, 628−635.
10. Boesze-Battaglia, K., Albert, A. D., and Yeagle, P. L. (1992) Fusion between disk membranes and plasma membrane of bovine photoreceptor cells is calcium dependent, *Biochemistry 31*, 3733−3738.
11. Boesze-Battaglia, K., Kong, F., Lamba, O. P., Stefano, F. P., and Williams, D. S. (1997) Purification and light-dependent phosphorylation of a candidate fusion protein, the photoreceptor cell peripherin/rds, *Biochemistry 36*, 6835−6846.
12. Boesze-Battaglia, K., Lamba, O. P., Jr., A. A. N., Sinha, S., and Guo, Y. (1998) Fusion between retinal rod outer segment membranes and model membranes: a role for photoreceptor peripherin/rds, *Biochemistry 37*, 9477−9487.
13. Primakoff, P., and Myles, D. G. (2002) Penetration, adhesion, and fusion in mammalian sperm-egg interaction, *Science 296*, 2183−2185.
14. Boesze-Battaglia, K., Goldberg, A., Dispoto, J., Katragadda, M., Cesarone, G., and Albert, A. (2003) A soluble peripherin/Rds C-terminal polypeptide promotes membrane fusion and changes conformation upon membrane association, *Exp. Eye Res. 77*, 505−514.
15. Frangioni, J. V., and Neel, B. G. (1993) Solubilization and purification of enzymatically active glutathione S-transferase (pGEX) fusion proteins, *Anal. Biochem. 210*, 179−187.
16. Gill, S. C., and von Hippel, P. H. (1989) Calculation of protein extinction coefficients from amino acid sequence data, *Anal. Biochem. 182*, 319−326.
17. Lauterwein, J., Bosch, C., Brown, L. R., and Wuthrich, K. (1979) Physiochemical studies of the protein-lipid interaction in melittin-containing micelles, *Biochim. Biophys. Acta 2*, 244−264.
18. Vinogradova, O., Sonnichsen, F., and Sanders, C. R. I. (1998) On choosing a detergent for solution NMR studies of membrane proteins, *J. Biomol. NMR 4*, 381−386.
19. Kyte, J., and Doolittle, R. F. (1982) A simple method for displaying the hydropathic character of a protein, *J. Mol. Biol. 157*, 105−132.
20. Wallace, B. A., and Janes, R. W. (1999) Tryptophans in membrane proteins, *Adv. Exp. Med. Biol. 467*, 789−799.
21. Baldwin, J. M. (1993) The probable arrangement of the helices in G protein-coupled receptors, *EMBO J. 12*, 1693−1703.
22. Delaglio, F., Grzesiek, S., Vuister, G. W., Zhu, G., Pfeifer, J., and Bax, A. (1995) NMRPipe: a multidimensional spectral processing system based on UNIX pipes, *J Biomol. NMR 6*, 277−293.
23. Alexandrescu, A. T., Abeygunawardana, C., and Shortle, D. (1994) Structure and dynamics of a denatured 131-residue fragment of staphylococcal nuclease: a heteronuclear NMR study, *Biochemistry 33*, 1063−1072.
24. Muller-Weeks, S., Boesze-Battaglia, K., and Fitzgerald, C. (2002) Deletional analysis of the rod photoreceptor cell peripherin/RDS carboxy-terminal region, *Exp. Eye Res. 75*, 143−154.
25. Albert, A. D., Goldberg, A. F. X., Katragadda, M., and Boesze-Battaglia, K. (2002) Interaction with the lipid surface induces a conformational change in the C-terminal region of peripherin/rds, *Invest. Ophthalmol. Visual Sci. 43*, 1398.

26. Boesze-Battaglia, K., Goldberg, A. F., Dispoto, J., Katragadda, M., Cesarone, G., and Albert, A. D. (2003) A soluble peripherin/Rds C-terminal polypeptide promotes membrane fusion and changes conformation upon membrane association, *Exp. Eye Res. 77*, 505−514.
27. Damek-Poprawa, M., Krouse, J., Gretzula, C., and Boesze-Battaglia, K. (2005) A novel tetraspanin fusion protein, peripherin-2, requires a region upstream of the fusion domain for activity, *J. Biol. Chem. 280*, 9217−9224.
28. Ritter, L. M., Arakawa, T., and Goldberg, A. F. (2005) Predicted and measured disorder in peripherin/rds a retinal tetraspanin, *Protein Pept. Lett. 12*, 677−686.
29. Jaroniec, C. P., Kaufman, J. D., Stahl, S. J., Viard, M., Blumenthal, R., Wingfield, P. T., and Bax, A. (2005) Structure and dynamics of micelle-associated human immunodeficiency virus gp41 fusion domain, *Biochemistry 44*, 16167−16180.
30. Lai, A. L., Park, H., White, J. M., and Tamm, L. K. (2006) Fusion peptide of influenza hemagglutinin requires a fixed angle boomerang structure for activity, *J. Biol. Chem. 281*, 5760−5670.
31. Cheng, S. F., Wu, C. W., Kantchev, E. A., and Chang, D. K. (2004) Structure and membrane interaction of the internal fusion peptide of avian sarcoma leukosis virus, *Eur. J. Biochem. 271*, 4725−4736.
32. Boesze-Battaglia, K., Lamba, O. P., Napoli, A. A. J., Sinha, S., and Guo, Y. (1998) Fusion between retinal rod outer segment membranes and model membranes: a role for photoreceptor peripherin/rds, *Biochemistry 37*, 9477−9487.
33. Boesze-Battaglia, K., Stefano, F. P., Fenner, M., Jr., and Napoli, A. A., Jr. (2000) A peptide analogue to a fusion domain within photoreceptor peripherin/rds promotes membrane adhesion and depolarization, *Biochim. Biophys. Acta 1463*, 343−354.
34. Wishart, D. S., Sykes, B. D., and Richards, F. M. (1992) The chemical shift index: a fast and simple method for the assignment of protein secondary structure through NMR spectroscopy, *Biochemistry 31*, 1647−1651.
35. Vinogradova, O., Sonnichsen, F., and Sanders, C. R., II. (1998) On choosing a detergent for solution NMR studies of membrane proteins, *J. Biomol. NMR 11*, 381−386.
36. Kitadokoro, K., Bordo, D., Galli, G., Petracca, R., Falugi, F., Abrignani, S., Grandi, G., and Bolognesi, M. (2001) CD81 extracellular domain 3D structure: insight into the tetraspanin superfamily structural motifs, *EMBO J. 20*, 12−18.
37. Moritz, O. L., and Molday, R. S. (1996) Molecular cloning, membrane topology, and localization of bovine rom-1 in rod and cone photoreceptor cells, *Invest. Ophthalmol. Visual Sci. 37*, 352−362.
38. Dyson, H. J., and Wright, P. E. (2005) Intrinsically unstructured proteins and their functions, *Nat. Rev. Mol. Cell Biol. 6*, 197−208.
39. Uversky, V. N. (2002) Natively unfolded proteins: a point where biology waits for physics, *Protein Sci. 11*, 739−756.
40. Tompa, P. (2002) Intrinsically unstructured proteins, *Trends Biochem. Sci. 27*, 527−533.
41. Boesze-Battaglia, K., Song, H., Sokolov, M., Lillo, C., Pankoski-Walker, L., Gretzula, C., Gallagher, B., Rachel, R. A., Jenkins, N. A., Copeland, N. G., Morris, F., Jacob, J., Yeagle, P., Williams, D. S., and Damek-Poprawa, M. (2007) The tetraspanin protein, peripheirn-2, complexes with melanoregulin, a putative membrane fusion regulator, *Biochemistry 46*, 1256−1272.
42. Tam, B. M., Moritz, O. L., and Papermaster, D. S. (2004) The C terminus of peripherin/rds participates in rod outer segment targeting and alignment of disk incisures, *Mol. Biol. Cell 15*, 2027−2037.
43. Batra-Safferling, R., Abarca-Heidemann, K., Korschen, H. G., Tziatzios, C., Stoldt, M., Budyak, I., Willbold, D., Schwalbe, H., Klein-Seetharaman, J., and Kaupp, U. B. (2006) Glutamic acid-rich proteins of rod photoreceptors are natively unfolded, *J. Biol. Chem. 281*, 1449−1460.
44. Poetsch, A., Molday, L. L., and Molday, R. S. (2001) The cGMP-gated channel and related glutamic acid-rich proteins interact with peripherin-2 at the rim region of rod photoreceptor disc membranes, *J. Biol. Chem. 276*, 48009−48016.
45. Lamb, R. A. (1983) In *Genetics of Influenza Viruses* (Paleae, P., and Kingsbury, D. W., Eds.) pp 21−69, Springer-Verlag, Heidelberg, Germany.
46. Lear, J. D., and DeGrado, W. F. (1987) Membrane binding and conformational properties of peptides representing the NH2 terminus of influenza HA-2, *J. Biol. Chem. 262*, 6500−6505.

BI061820C